



Title	Revisiting the Origins of the Fracture Energy of Tough Double-Network Hydrogels with Quantitative Mechanochemical Characterization of the Damage Zone
Author(s)	Matsuda, Takahiro; Kawakami, Runa; Nakajima, Tasuku; Hane, Yukiko; Gong, Jian Ping
Citation	Macromolecules, 54(22), 10331-10339 <a href="https://doi.org/10.1021/acs.macromol.1c01214">https://doi.org/10.1021/acs.macromol.1c01214</a>
Issue Date	2021-11-23
Doc URL	<a href="http://hdl.handle.net/2115/87284">http://hdl.handle.net/2115/87284</a>
Rights	This document is the Accepted Manuscript version of a Published Work that appeared in final form in Macromolecules, copyright © American Chemical Society after peer review and technical editing by the publisher. To access the final edited and published work see <a href="https://pubs.acs.org/articlesonrequest/AOR-NTMZZIC6JF31XUMVZWPZ">https://pubs.acs.org/articlesonrequest/AOR-NTMZZIC6JF31XUMVZWPZ</a> .
Type	article (author version)
Additional Information	There are other files related to this item in HUSCAP. Check the above URL.
File Information	Macromolecules 54-22_10331-10339.pdf



[Instructions for use](#)

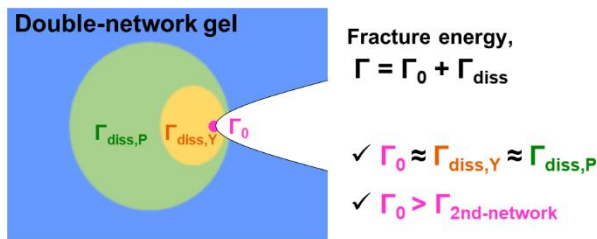
# Revisiting the origins of the fracture energy of tough double-network hydrogels with quantitative mechanochemical characterization of the damage zone

Takahiro Matsuda<sup>\*‡</sup>, Runa Kawakami<sup>†</sup>, Tasuku Nakajima<sup>‡,§</sup>, Yukiko Hane<sup>§</sup>, and Jian Ping Gong<sup>\*‡,§</sup>

<sup>‡</sup>Faculty of Advanced Life Science, Hokkaido University, N21W11, Kita-ku, Sapporo 001-0021, Japan. <sup>†</sup>Graduate School of Life Science, Hokkaido University, N21W11, Kita-ku, Sapporo 001-0021, Japan. <sup>§</sup>Institute for Chemical Reaction Design and Discovery (WPI-ICReDD), Hokkaido University, N21W10, Kita-ku, Sapporo 001-0021, Japan.

\*Corresponding authors: [tkhr.matsuda@gmail.com](mailto:tkhr.matsuda@gmail.com), [gong@sci.hokudai.ac.jp](mailto:gong@sci.hokudai.ac.jp)

Table of Contents (TOC) graphic (For Table of Contents use only)



## ABSTRACT

The high fracture energy of tough soft materials can be attributed to the large energy dissipation zone around the crack tip. Hence, quantitative characterization of energy dissipation is key to soft matter fracture mechanics. In this study, we quantified the energy dissipation in the damage zone of a double-network (DN) hydrogel using a mechanochemical technique based on mechanoradical polymerization combined with confocal fluorescence microscopy. We found that, in addition to energy dissipation in a relatively narrow yield region, the dissipation in the wide pre-yielding region and the intrinsic fracture energy also have large contribution to the fracture energy. Moreover, the fracture energy of a pre-stretched sample, in which the dissipative capacity is nearly depleted, suggests that the intrinsic fracture energy is higher than the fracture energy of the second network. These findings modify the previous understanding that the fracture energy of DN gels is dominated by the energy of the yielding zone formation.

## INTRODUCTION

The fracture toughness, that is, the crack resistance of materials under mechanical stress, is an important aspect in ensuring the performance of materials in real applications. Toughening soft materials, such as gels and elastomers, and the related fracture mechanics are gaining considerable interest recently.<sup>1-7</sup> Research on these topics has been pushed by the development of various tough soft materials in recent decades<sup>8-15</sup> and also by emerging applications, such as soft wearable devices and biomedical implants.<sup>16-19</sup> The toughness of soft materials is typically characterized as the fracture energy  $\Gamma$ , in units of  $\text{J m}^{-2}$ , which represents the energy required to increase the length of a crack into forming a unit area of the fractured surface. The fracture energy  $\Gamma$  of tough soft materials has two contributions:<sup>1,2,6,7,20</sup>

$$\Gamma = \Gamma_0 + \Gamma_{\text{diss}} \quad (1)$$

where  $\Gamma_0$  represents the intrinsic fracture energy directly related to the material separation at the crack tip, and  $\Gamma_{\text{diss}}$  represents the dissipation that occurs in the process zone around the crack tip, whose size typically ranges from sub-micrometers to centimeters in soft materials. The dissipation mechanism includes microstructural destruction and viscoelastic dissipation, depending on the structure of the material. For most tough soft materials,  $\Gamma_{\text{diss}}$  is considered to be much larger than  $\Gamma_0$ , so that the overall fracture energy  $\Gamma$  can be approximated as  $\Gamma \approx \Gamma_{\text{diss}}$ .<sup>1,6,20,21</sup> Therefore, elucidating the dissipation mechanism in the process zone and its quantitative understanding are central topics in understanding the fracture mechanics of soft materials.

As part of the efforts to make tough soft materials, the double-network (DN) concept<sup>9,22</sup> has been widely applied to hydrogels and elastomers comprising polymer networks with various

chemical features.<sup>9,10,12,22–28</sup> Specifically, a DN gel is composed of interpenetrated two contrasting polymer networks: one, a brittle and sparse network (called *the first network*, typically 1–5 wt.%) and the other, a stretchable and dense network (called *the second network*, typically 10–20 wt.%).<sup>22</sup> Even when comprising 80–90 wt.% water, DN gels show extremely high fracture energies of 300–5000 J m<sup>-2</sup>, which is one or two orders of magnitude higher than that of conventional single-network hydrogels.<sup>29–31</sup>

The toughening mechanism of DN gels has been extensively investigated. Findings on the yielding that often accompanies necking,<sup>32,33</sup> strain rate-insensitive stress–strain relations, and irreversible mechanical hysteresis<sup>28,34–36</sup> in DN gels suggest an *internal fracturing* mechanism. When a DN gel is stressed, the brittle first network breaks, whereas the stretchable second network can maintain the integrity of the material. The covalent bond scission of the polymer strands was recently verified by chemical sensing of mechanoradicals.<sup>37</sup> Internal fracturing suggests that the extraordinarily high fracture energy of DN gels can be attributed to the formation of a *damage zone* around the crack tip, in which the brittle first network breaks owing to stress concentration.<sup>20,21,35,38</sup> In the damage zone, a large amount of mechanical energy,  $\Gamma_{\text{diss}}$  in **Eq. (1)**, dissipates prior to crack progression. Therefore, a quantitative comparison of  $\Gamma_{\text{diss}}$  caused by internal fracturing in the damage zone with the apparent fracture energy  $\Gamma$  is indispensable for clarifying the fracture mechanism of DN gels.

Quantitative characterization of the energy dissipation in DN gels upon fracture, however, has been a challenge owing to lack of suitable techniques. Although the damage zone was first observed by optical microscopes,<sup>35,39</sup> these techniques do not provide quantitative information on the distribution of internal fractures. Recently, mechanochemical techniques for visualizing and

quantifying stress, strain, and internal fractures around the crack tip of DN gels and multiple-network elastomers have been reported.<sup>12,40-42</sup> For DN gels, we developed a method using mechanoradicals generated by homolytic polymer strand scission of the first network in the damage zone in order to initiate a polymerization of the *N*-isopropylacrylamide (NIPAAm) monomers preloaded in the DN gel, which formed a thermoresponsive polymer PNIPAAm tethered to the broken ends of the first network strands.<sup>40</sup> The distribution of PNIPAAm was then visualized with laser-scanning confocal microscopy (LSCM) using a pre-loaded environment-responsive fluorophore at a temperature above the lower critical solution temperature (LSCT) of PNIPAAm. The spatial distributions of stress, strain, and dissipated mechanical energy density around the crack tip were quantified using a calibration curve obtained from the fluorescence intensities of uniaxially stretched tensile specimens.

In this study, we compared the total energy dissipation in the damage zone as measured by the mechanoradical polymerization method with the fracture energy of a DN gel. We found that the dissipated energy in the damage zone per unit of fractured surface area was distinctly smaller than the fracture energy measured by the tearing fracture test. This finding suggests that the intrinsic fracture energy  $\Gamma_0$  is not negligible for this DN gel. This presumption is further confirmed by measuring the fracture energies of a polyacrylamide single-network gel as a model of the second network and of a pre-stretched DN gel in which dissipation capacity was depleted.

## EXPERIMENTS

**Materials.** The DN gel used in this paper was synthesized via a two-step polymerization following the method used in our previous work.<sup>40</sup> The feed concentrations of the monomer (2-acrylamido-2-methylpropane sulfonic acid sodium salt; NaAMPS), crosslinker (*N,N'*-methylenebisacrylamide; MBAA), and radical initiator (2-oxoglutaric acid; OA) for the first network were 1.0 M, 30 mM (3 mol%, with respect to the monomer), and 10 mM (1 mol%), respectively, and the feed concentrations of the monomer (acrylamide; AAm), crosslinker (MBAA) and radical initiator (OA) for the second network were 4.0 M, 0.8 mM (0.02 mol%), and 0.4 mM (0.01 mol%), respectively. Ultraviolet light ( $\sim 365$  nm,  $4$  mW cm<sup>-2</sup>) irradiation times for the first and second network polymerizations were 8 h and 9 h, respectively. The synthesized DN gel was immersed in a large volume of deionized water for at least 1 day to allow the gel to equilibrate. Due to the large amount of initiator (1 mol% with respect to the monomer) in the first-network synthesis, one-end unreacted crosslinkers were almost inactivated; hence, the number of inter-connections between the first and second networks could be negligibly small.<sup>43</sup> The negligible inter-connections between the first and second networks of the DN gel allowed us to estimate the fracture energy of the second network using the value determined from a PAAm single-network hydrogel. A polyacrylamide (PAAm) single-network hydrogel was synthesized with the same formulation as that of the second network (4.0 M AAm, 0.8 mM MBAA, and 0.4 mM OA). The as-prepared PAAm gel (PAAm concentration of 28 wt.%), with a weight of  $w$  (g) ( $w = 5.40$ – $5.63$  g), was swollen with  $0.65w$  (g) of water, resulting in a “controlled-swollen PAAm gel” that had the same PAAm concentration (17 wt.%) as the DN gel. Note that the controlled-swollen PAAm gel is not at the equilibrium swollen state in water.

**Tensile test.** Uniaxial tensile test was performed following a previously reported procedure.<sup>37,40</sup> Briefly, a dumbbell-shaped sample (gauge length 12 mm) was stretched using a tensile tester (INSTRON 5965, Instron Co.) at a crosshead velocity of 100 mm min<sup>-1</sup>. Strain  $\varepsilon$  was measured using a non-contact video extensometer (AVE, Instron Co.).

**Tearing fracture test.** To characterize the tearing fracture energies  $\Gamma$  of the DN gel and PAAm gels, a trouser-type tearing fracture test was carried out.<sup>6,44,45</sup> A trouser-shaped sample (thickness  $t = 3.1$  mm for the DN gel and  $t = 1.2$  mm for the PAAm gel, full width 8.0 mm, each leg's width  $w = 4.0$  mm, full length  $\sim 50$  mm, and initial cut length  $\sim 20$  mm, see **Figure S1**) was torn at the crosshead velocity of 100 mm min<sup>-1</sup> using a tensile tester (INSTRON 5965). During tearing, the elongation of the leg was measured using a video extensometer (AVE, Instron Co.) (**Figure S1**).<sup>27</sup> The tearing fracture energy  $\Gamma$  was calculated as:<sup>6</sup>

$$\Gamma = \frac{2F_c\lambda_c}{t} - 2wW_c \quad (2)$$

where  $F_c$ ,  $\lambda_c$ , and  $W_c$  are the average force, average elongation ratio of the leg, and average strain energy density of the leg, respectively, during crack propagation.

**Single-edge notch fracture test.** Single-edge notch fracture test was carried out to characterize the fracture energy of the DN gel, the PAAm gels, and the pre-stretched DN gel. The detailed procedure is provided in **Supporting Note I** in the SI. Briefly, we used dumbbell-shaped samples (gauge length 25 mm, width 4 mm, and thickness 1.0–1.7 mm) with a  $\sim 1.0$  mm notch made using a razor blade. The notch length was measured for each individual specimen. The notched sample was stretched at a crosshead velocity of 100 mm min<sup>-1</sup> until rupture. The fracture



energy from the single-edge notch test was determined as the critical energy release rate at the onset of the crack propagation,  $G_c$ , as follows:<sup>4,6,46</sup>

$$G_c = 2kW_c c_0 = \frac{6W_c c_0}{\sqrt{\lambda_c}} \quad (3)$$

where  $c_0$  is the initial notch length,  $W_c$  and  $\lambda_c$  are the strain energy density and elongation ratio at the onset of crack propagation, respectively, and  $k$  is the prefactor (assumed to be  $k =$

$3\lambda^{1/2}$ ).<sup>4,6,46,47</sup> To measure the  $G_c$  of a DN gel pre-stretched to the point close to its failure, an un-notched DN gel was first stretched to an elongation ratio  $\lambda = 6.0$ , and then unloaded.

Subsequently, a notch (approximately 1.0 mm) was inserted on this pre-stretched DN sample.

The pre-stretched and notched DN gel was stretched until rupture to determine  $G_c$ .

**Damage zone characterization.** The damage zone of a torn DN gel was visualized and characterized using a mechanoradical polymerization of NIPAAm, fluorescent molecule 8-anilino-1-naphthalenesulfonic acid (ANS), and laser-scanning confocal microscopy, as previously reported.<sup>40</sup> Briefly, a trouser-shaped DN gel containing 1.0 M NIPAAm and 200 mg mL<sup>-1</sup> ANS was torn at a crosshead velocity of 100 mm min<sup>-1</sup> in a glove box under argon atmosphere at ~15 °C. The torn gel was wrapped with a plastic film to prevent drying, followed by incubation in a glove box for ~18 h. Fluorescence microscopic measurements were carried out at 42 °C (above the LSCT of NIPAAm) using a laser scanning confocal microscope (Nikon A1 Rsi and Ti-E, Nikon Co.) equipped with a Plan Fluor x4 objective lens (NA 0.13, Nikon Co.). The excitation laser wavelength was 402.5 nm. All measurements were performed at the depth of 5 μm from the sample surface. The same laser intensity was used for all measurements. The theoretical spatial resolutions in the observation plane and in the depth direction were ~1.4 μm

and  $\sim 50 \mu\text{m}$ , respectively, which gave the ellipsoidal volume of  $\sim 50 \mu\text{m}^3$  for each measured point. Fluorescence intensities were measured at a  $6.2 \mu\text{m}$  interval. The obtained data was moving-averaged over 9 data points to smooth out the experimental noise.<sup>40</sup> The data processing procedure was performed as reported in the previous study.<sup>40</sup>

The fluorescence intensity of the torn sample was converted into the energy dissipation density using the calibration curve obtained from uniaxially-stretched specimens of the DN gel.<sup>40</sup> The concentrations of NIPAAm (1.0 M) and ANS ( $200 \text{ mg mL}^{-1}$ ) and all LSCM conditions (equipment, temperature, resolutions and excited volume, laser intensity, and measured depth from the sample surface) used for the tensile samples were the same for the torn sample. The identical conditions allowed to compare the fluorescence intensity of the stretched samples to that of the torn sample.

## Results

### Tensile properties and tearing fracture energy

The DN gel adopted in this work showed a yielding and strain-hardening phenomena under uniaxial tensile testing (**Figure 1a**). Note that the stress yielding of DN gels does not accompany plastic deformation. In fact, common DN gels exhibit a small residual strain of only 5–20% even after experiencing a large strain of 200–1000%.<sup>30,36</sup> The yielding of this DN gel did not accompany explicit necking deformation,<sup>32,33,48,49</sup> and the gel deformed homogeneously even above the yielding point.<sup>49</sup>

Fracture energy of the DN gel was characterized by trouser-tearing test because the tearing fracture energy can be determined by an energy balance equation regardless of the bulk dissipation history and without using any empirical parameters.<sup>6,44–47</sup> Under the tearing test, the DN gel showed stable (i.e., no stick-slip) crack propagation (**Figure 1b**), during which the strain of the sample leg far from the crack was as small at  $\varepsilon_c \sim 0.14$  (**Figure 1c**), which is below the threshold strain for mechanical hysteresis. The average tearing force was  $F_c = 1.45$  N, and the average elongation ratio and energy density of the leg were  $\lambda_c = \varepsilon_c + 1 = 1.14$ , and  $W_c = 9.3$  kJ  $\text{m}^{-3}$ , respectively, resulting in a tearing fracture energy of  $\Gamma = 991$  J  $\text{m}^{-2}$  based on **Eq. (2)**.

Averaged over four measurements, the  $\Gamma$  of this DN gel was determined to be  $906 \pm 62$  J  $\text{m}^{-2}$  (with standard deviation), which lies in the normal range for DN gels synthesized in various compositions (typically 300–5000 J  $\text{m}^{-2}$ ).<sup>30,31</sup>

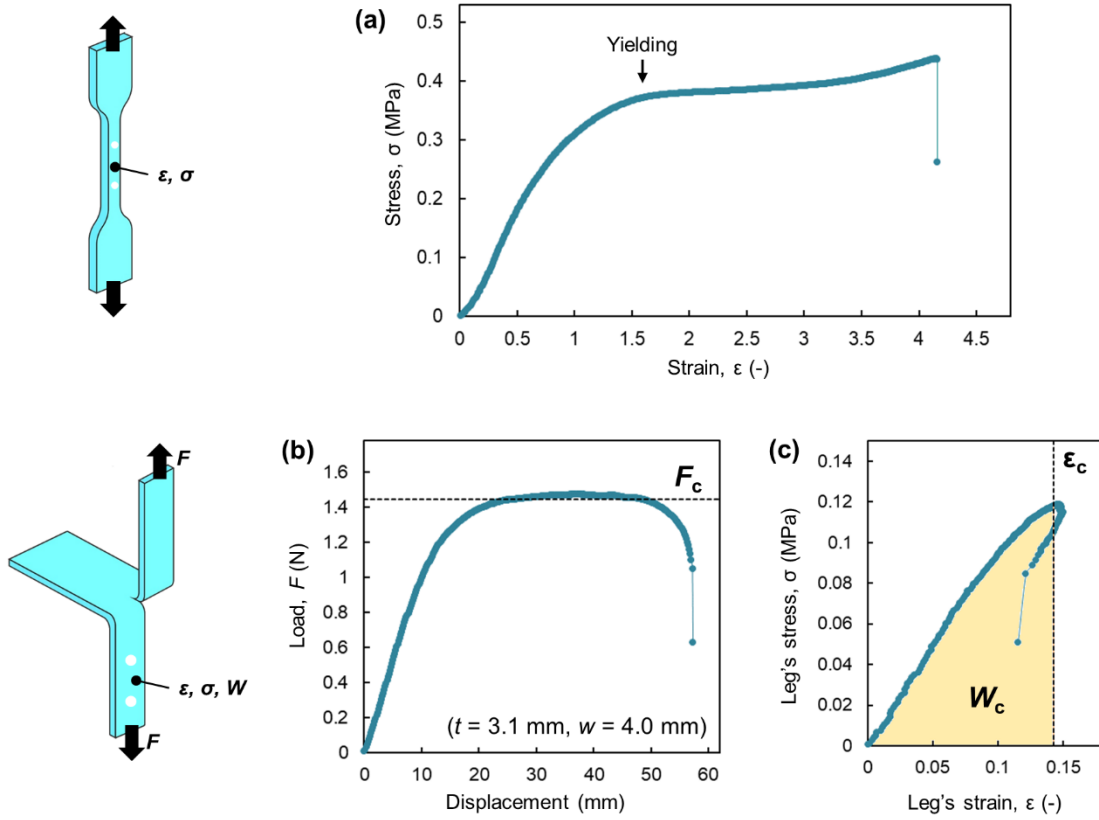


**Figure 1.** Tensile test and trouser-tearing fracture test of the DN gel. **(a)** Stress–strain curve under uniaxial tensile test using a dumbbell-shaped specimen (data reproduced from Ref. 40). **(b)** Force–displacement curve of a trouser-shaped specimen during the fracture test. **(c)** Stress–strain curve of a leg of the trouser sample far from the crack tip during the fracture test. The leg strain was measured by a non-contact video extensometer.

## Energy dissipation in the damage zone of the DN gel

As reported in our previous paper, the mechanoradical polymerization technique combined with fluorescent molecules and LSCM enables the determination of the profiles of the dissipated energy density  $U_{\text{diss}}$  ( $\text{J m}^{-3}$ ) around the fractured surface of DN gels using a calibration curve obtained from the fluorescence intensities of uniaxially stretched tensile specimens.<sup>40</sup> The potential differences between the fluorescence intensities in tearing fracture and uniaxial stretching are described later in Discussion and **Supporting Note II**.

Herein, we set the  $(x,y,z)$  coordinates of a fractured sample obtained from the trouser-tearing test, as illustrated in **Figure 2a**. The two-dimensional LSCM image of the  $x$ - $z$  plane of a torn DN gel (**Figure 2b**) shows that the fluorescence intensity was maximized at the fractured surface ( $z = 0$ ) and gradually decreased along the  $z$  direction, indicating the distribution of the degree of internal fracturing. Note that the maximum fluorescence intensity near the fracture surface in the torn sample is almost the same as that of the yielding point in the uniaxially stretched sample, indicating that most of the observed damage zone is pre-yielding region. Using the calibration curve obtained from tensile specimens (**Figure 2c**), the fluorescence intensity of the fractured sample was converted into dissipated energy density  $U_{\text{diss}}$ .<sup>40</sup> The profile of the internal energy dissipation density  $U_{\text{diss}}$  ( $\text{J m}^{-3}$ ) as a function of the distance from the fractured surface to the bulk,  $z$ , is shown in **Figure 2d**.

Since the reports by Brown<sup>21</sup> and Tanaka<sup>20</sup> on fracture models of DN gels in 2007, it has been considered that the high fracture toughness of the DN gel can be predominantly attributed to the dissipated mechanical energy in the damaged zone,  $\Gamma_{\text{diss}}$ .<sup>1,6,20-23</sup> Some previous reports simply estimated it as  $\Gamma_{\text{diss}} = 2hU_{\text{diss}}$ , where  $h$  is the damage zone size, and the numerical factor 2

corresponds to two symmetric fractured surfaces being formed.<sup>35,39</sup> This approximation was constructed under the assumption of a homogeneous dissipated energy density  $U_{\text{diss}}$  in the damage zone. In contrast, our results indicate that  $U_{\text{diss}}$  is not homogeneous along the  $z$ -direction, as shown in **Figure 2d**. In these cases,  $\Gamma_{\text{diss}}$  is estimated by integration,<sup>6,7</sup>

$$\Gamma_{\text{diss}} = 2 \int_0^h U_{\text{diss}}(z) dz, \quad (4)$$

under an assumption that the dissipation is independent on the  $y$ -coordinate. The integration ( $\Gamma_{\text{diss}}/2 = \int_0^h U_{\text{diss}} dz$ ) is indicated as the highlighted area under the  $U_{\text{diss}}-z$  curve at  $0 < z < h$  in **Figure 2d**. We set the damage zone size to  $h = 1500$  mm, at which point the fluorescence intensity reached the background level. From the integration, the  $\Gamma_{\text{diss}}$  of the DN gel was calculated to be  $307 \pm 6$  J m<sup>-2</sup>.  $\Gamma_{\text{diss}}$  thus obtained is of the same order of magnitude as the fracture energy  $\Gamma$  ( $\sim 900$  J m<sup>-2</sup>) but considerably smaller.

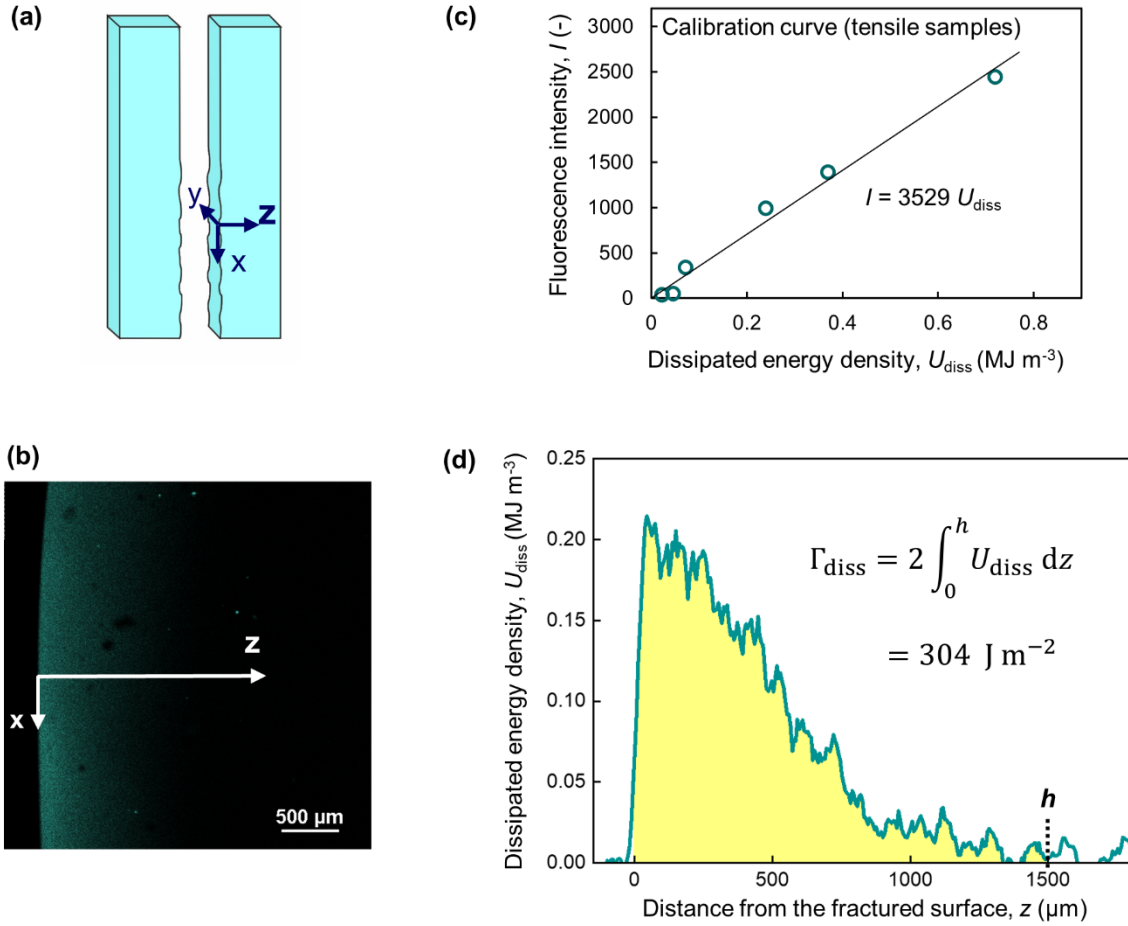


**Figure 2.** Characterization of the dissipated mechanical energy in the damage zone,  $\Gamma_{\text{diss}}$ , of a torn sample by the trouser-tearing test. **(a)** Schematic illustration of a fractured DN gel and the  $(x,y,z)$  coordinates. **(b)** Fluorescence intensity image in  $x$ - $z$  plane of a fractured DN gel obtained by LSCM. **(c)** Calibration curve of fluorescence intensity  $I$  and dissipated energy density  $U_{\text{diss}}$ , obtained from tensile specimens, with a linear regression ( $I = 3529U_{\text{diss}}$ ) that is used as a calibration curve to convert  $I$  into  $U_{\text{diss}}$  of the torn sample. **(d)** Dissipated energy density profile along the  $z$ -axis from the torn surface to the bulk, obtained from the fluorescence intensity profile. The energy dissipation in the damage zone,  $\Gamma_{\text{diss}}$ , is obtained by integrating  $U_{\text{diss}}$  along the  $z$ -axis from 0 to 1500  $\mu\text{m}$  multiplied by 2. From six measurements of the individual positions, we obtained  $\Gamma_{\text{diss}} = 307 \pm 6 \text{ J m}^{-2}$ . Figures 2c and 2d are reproduced based on data published previously.<sup>40</sup>

## Origins of the fracture energy

As described in the Introduction, the fracture energy of a tough soft material  $\Gamma$  is characterized as  $\Gamma = \Gamma_{\text{diss}} + \Gamma_0$ , where  $\Gamma_0$  is the intrinsic fracture energy at the crack tip. Theoretical models proposed by Brown and Tanaka on the fracture toughness of DN gels suggested  $\Gamma \approx \Gamma_{\text{diss}}$  ( $\gg \Gamma_0$ ).<sup>20,21</sup> However, our results indicate that  $\Gamma$  ( $\sim 900 \text{ J m}^{-2}$ ) is considerably larger than  $\Gamma_{\text{diss}}$  ( $\sim 300 \text{ J m}^{-2}$ ). This large discrepancy can be attributed to (1) an underestimation of the dissipated energy at the yield region close to the fractured surface and (2) non-negligible  $\Gamma_0$ .

**(i) Dissipated energy in damage zone.** First, we considered whether the dissipated energy  $\Gamma_{\text{diss}}$  was underestimated. Although our method clearly detected the broad non-yield region in which the applied strain was  $0.5 < \varepsilon < 1.6$  ( $z$  ranging up to  $\sim 1500 \mu\text{m}$ ), a narrow yield region ( $\varepsilon > 1.6$ , expected to range up to  $\sim 100 \mu\text{m}$  for  $z$ ) was not properly characterized owing to the limited measurement resolution of the current LSCM setup.<sup>40</sup> The size of the yield region of  $\sim 100 \mu\text{m}$  is also as expected from a previous study by Liang et al., in which a  $150\text{--}300 \mu\text{m}$  yield region was observed for a thin DN gel in its reswollen state.<sup>39</sup> Because yielded DN gels further swell to approximately two times the length due to internal fracturing,<sup>36,50</sup> the size of the yielding zone was re-evaluated to being approximately  $75\text{--}150 \mu\text{m}$ . Although the composition and thickness of the DN gel by Liang et al. were slightly different from our DN gel, the yielding zone size of our DN gel is expected to be approximately  $100 \mu\text{m}$ .

Dissipation in the yielding zone has been considered as the dominant contribution to the fracture energy, because the energy dissipation density in the yielding zone is more significant than the



pre-yielding zone. In the yielding zone, the dissipated energy density  $U_{\text{diss}}$  of this DN gel is approximately  $1.0 \text{ MJ m}^{-3}$  at maximum.<sup>40</sup> Therefore, dissipated energy per unit of fractured area in the yielding zone is approximately estimated as  $1.0 \text{ MJ m}^{-3} \times (1.0 \times 10^{-4} \text{ m}) = 100 \text{ J m}^{-2}$  at maximum. However, this value hardly explains the discrepancy between  $\Gamma_{\text{diss}}$  characterized by integration ( $\sim 300 \text{ J m}^{-2}$ ) and  $\Gamma$  characterized by a tearing fracture test ( $\sim 900 \text{ J m}^{-2}$ ). This estimation also indicates that the energy dissipation in the pre-yielding zone ( $\sim 300 \text{ J m}^{-2}$ ) contributes similarly or more than that in the yielding zone ( $\sim 100 \text{ J m}^{-2}$ ) because of the larger dissipation volume in the pre-yielding zone.

**(ii) Intrinsic fracture energy,  $\Gamma_0$ .** Next, the intrinsic fracture energy,  $\Gamma_0$ , was examined.

Previously,  $\Gamma_0$  of DN gels has been considered as being identical to the fracture energy of the pure second network, and it has been assumed to be very small because the fracture energies of some chemically crosslinked PAAm gels are quoted as  $\sim 10 \text{ J m}^{-2}$  in the literature.<sup>20,21,51</sup> However, Suo and co-workers recently reported that the fracture energy of some loosely crosslinked PAAm gels, which is similar to the second network of our DN gel, is  $100\text{--}500 \text{ J m}^{-2}$ .<sup>3,10,52,53</sup> Therefore, the fracture energy of the second network  $\Gamma_{2\text{nd}}$  may not be negligible. Moreover, it is still an open question whether the intrinsic fracture energy  $\Gamma_0$  can be approximated by  $\Gamma_{2\text{nd}}$ .<sup>6</sup>

To re-examine  $\Gamma_{2\text{nd}}$  and  $\Gamma_0$ , we measured the fracture energy of the PAAm gel and a largely pre-stretched DN gel (see **Supporting Note I** and **Figures S2–S4** for details). The former was prepared using the same formulation (monomer AAm 4.0 M and crosslinker MBAA 0.8 mM) as for the second network of the DN gel, which was then swollen with a controlled amount of water to make the PAAm concentration the same for the DN gel at swollen state (17 wt.% PAAm). For the latter, we used a DN gel that was pre-stretched until close to its rupture point before the

fracture energy measurement. The fracture energy of the pre-stretched specimen is considered to be close to the  $\Gamma_0$  of the DN gel because many first network strands were ruptured during the first stretching, so that the dissipative capacity was nearly depleted, similar to a report by Zhang et al.<sup>54</sup>

Here, we used single-edge notch test to determine the fracture energy of the pre-stretched DN gel because of the anisotropic feature of the internal fracture of DN gels.<sup>36,50,55</sup> Considering the anisotropic internal fracture, the pre-stretching direction should be the same as the direction of principal stress in the following fracture test in order to deplete the dissipation capacity around the crack tip. For this reason, the single-edge notch test is technically more appropriate than the trouser-tearing test. We also measured the fracture energies of the virgin DN gel and the PAAm gel by single-edge notch test to compare directly with that of the pre-stretched DN gel. Although the fracture energy characterized from the single-edge notch test  $G_c$  does not have to be exactly identical to the trouser-tearing fracture energy  $\Gamma$ , these two values are in the same order of magnitude within a factor of  $\sim 2$  (for example, Ref. 44 for a vulcanized natural rubber, Ref. 27 for DN elastomers, and **Table 1** for the DN gel and PAAm gels).

The results are shown in **Figure 3** and **Table 1**. The  $G_c$  of the virgin DN gel was  $826 \pm 245 \text{ J m}^{-2}$ , which is close to the tearing fracture energy ( $906 \pm 62 \text{ J m}^{-2}$ ). For the controlled-swollen PAAm gel, fracture energy determined from single-edge notch test and trouser-tearing test are  $184 \pm 21 \text{ J m}^{-2}$  and  $168 \pm 54 \text{ J m}^{-2}$ , respectively. Hence,  $\Gamma_{2nd}$  ( $150\text{--}200 \text{ J m}^{-2}$ ) is not negligibly small compared with the fracture energy of the DN gel ( $\sim 900 \text{ J m}^{-2}$ ).

For the fracture energy measurement of the pre-stretched DN gel in which dissipation capacity was nearly depleted, the DN gel was first stretched to the elongation ratio  $\lambda = 6.0$  to induce

plenty of internal fracturing, and then, the sample was unloaded to the original length. The single-edge notch fracture test was then carried out on this pre-stretched sample by making a notch vertical to the pre-stretched direction (**Figure 3a**). Surprisingly, we found that the fracture energy of the pre-stretched DN gel (denoted as  $G_c^*$ ) is  $697 \pm 123 \text{ J m}^{-2}$ , which is much larger than the fracture energy of the second network (**Figure 3b**). This is also supported by the original stress–elongation ratio curves of the notched samples for these two gels. As shown in **Figure 3c**, the trajectories of the curves of the two notched gels were similar, but the rupture points differed significantly. This observation indicates a large difference in the fracture energy between the PAAm single-network gel and the pre-stretched DN gel. Although the  $G_c^*$  characterized herein must be slightly higher than the actual intrinsic fracture energy because some of the first network strands can break further with an increase in stretching, the result strongly suggests that the intrinsic fracture energy is higher than the fracture energy of the second network. Moreover, **Figure 3b** implies that intrinsic fracture energy may not be far from the fracture energy of the virgin DN gel.

**Table 1.** Fracture energies characterized by trouser-tearing test and single-edge notch test<sup>a</sup>

Sample	$\phi_{\text{PNaAMPS}}$ (wt.%)	$\phi_{\text{PAAm}}$ (wt.%)	$\Gamma$ (J/m <sup>2</sup> )	$G_c$ (J/m <sup>2</sup> )
virgin DN gel	2	17	$906 \pm 62$	$826 \pm 245$
pre-stretched DN gel <sup>b</sup>	2	17	not measured	$697 \pm 123$
as-prepared PAAm gel	-	28	$199 \pm 14$	$343 \pm 78$
controlled-swollen PAAm gel	-	17	$168 \pm 54$	$184 \pm 21$

<sup>a</sup>  $\phi_{\text{PNaAMPS}}$  and  $\phi_{\text{PAAm}}$  are the weight fractions of the PNaAMPS and PAAm, respectively.  $\Gamma$  and  $G_c$  are the fracture energies characterized by trouser-tearing test and single-edge notch test, respectively. Error ranges denote the standard deviations for 3–4 measurements. <sup>b</sup> Pre-stretch ratio  $\lambda = 6$ .

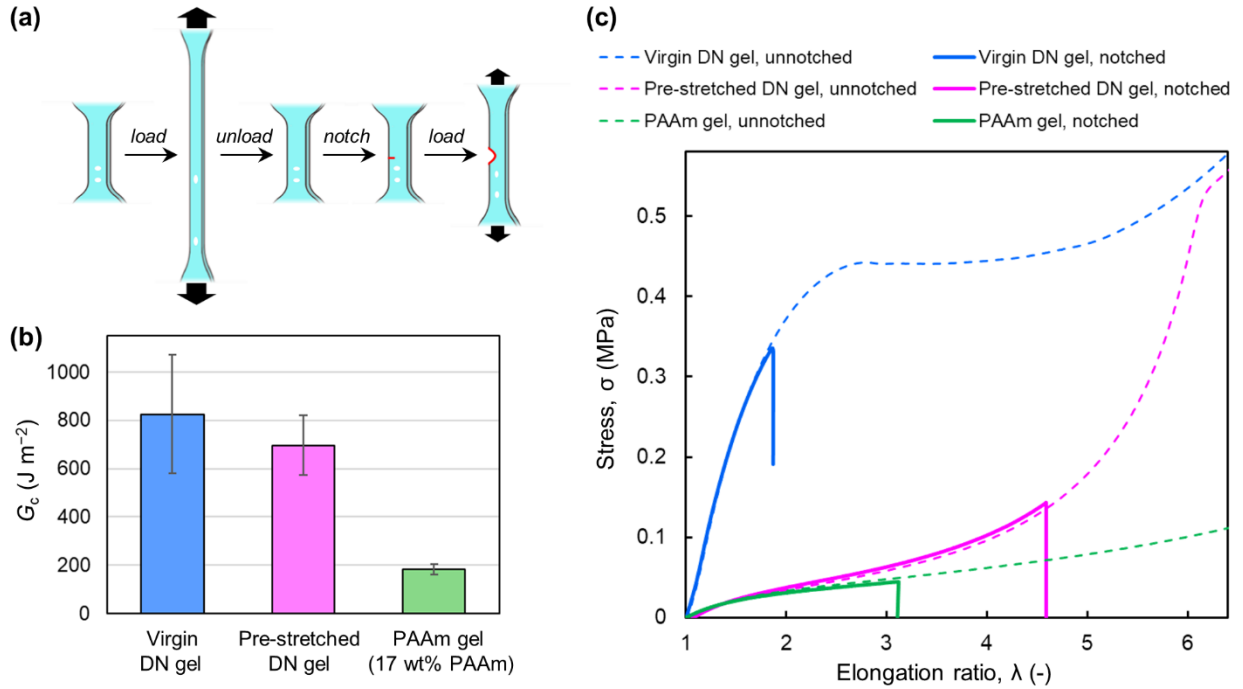


**Figure 3.** Fracture energy,  $G_c$ , measured by single-edge notch test. **(a)** Schematic illustration of the procedures for measuring the fracture energy of a pre-stretched DN gel with significant internal damage. A virgin DN gel is stretched to a strain close to its rupture point and then unloaded, followed by the fracture energy measurement of the pre-stretched gel by a single-edge notch test. **(b)** Fracture energy  $G_c$  of the virgin DN gel, the pre-stretched DN gel (pre-stretched ratio  $\lambda = 6$ ), and the controlled-swollen PAAm gel with a polymer weight fraction of 17 wt.% that was the same as the PAAm fraction in the DN gel. The error bars represent the standard deviation for 3–4 measurements. **(c)** Typical stress–elongation ratio curves of the notched (solid curves) and unnotched (dashed curves) samples of the virgin DN gel (blue), the pre-stretched DN gel (magenta), and the PAAm gel with a polymer weight fraction of 17 wt.% (green), with notch lengths of 1.03 mm, 0.97 mm, and 1.00 mm, respectively. To highlight the results of the notched samples, only parts of the curves are shown for the unnotched samples.

## Discussion

For the DN gel with a fracture energy of  $\Gamma = 900 \text{ J m}^{-2}$ , the fluorescence observation shows that the energy dissipation in the damage zone  $\Gamma_{\text{diss}}$  is approximately  $400 \text{ J m}^{-2}$  ( $\sim 300 \text{ J m}^{-2}$  in the pre-yielding zone and  $\sim 100 \text{ J m}^{-2}$  in the yielding zone), which predicts  $\Gamma_0$  of  $\sim 500 \text{ J m}^{-2}$ . The fluorescence method using mechanoradical polymerization can contain some uncertain method-specific errors (see **Supporting Note II** in the SI). Even so, individual fracture test results clearly indicate that  $\Gamma_0$  is as large as  $150\text{--}700 \text{ J m}^{-2}$ , which supports the prediction of  $\Gamma_0$  by the fluorescence observation. Taking the uncertain experimental errors into account, it can be concluded that the fracture energy  $\Gamma$  ( $\sim 900 \text{ J m}^{-2}$ ) of the DN gel is the sum of the energy dissipation  $\Gamma_{\text{diss}}$  in the pre-yielding and yielding zones of  $200\text{--}400 \text{ J m}^{-2}$  and  $50\text{--}300 \text{ J m}^{-2}$ , respectively, and the intrinsic fracture energy  $\Gamma_0$  of  $150\text{--}700 \text{ J m}^{-2}$  (**Figure 4**).

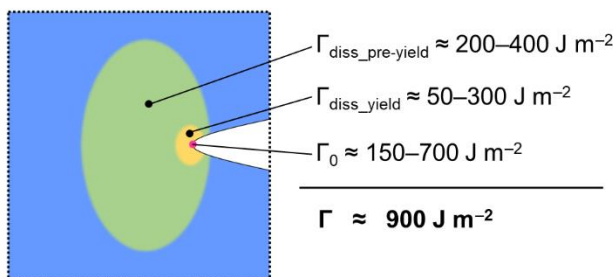


**Figure 4.** Schematic representation of the three contributions (dissipated energy in the wide pre-yielding zone  $\Gamma_{\text{diss\_pre-yeild}}$ , dissipated energy in the narrow yielding zone  $\Gamma_{\text{diss\_yeild}}$ , and intrinsic fracture energy  $\Gamma_0$ ) to the fracture energy  $\Gamma$  of the DN gel. For the DN gel used in this work, each of these three factors makes non-negligible contribution to the fracture energy of the DN gel.

Most studies on DN gels mainly, or only, considered energy dissipation in the yielding zone and assumed  $\Gamma \approx \Gamma_{\text{diss}} \gg \Gamma_0$ .<sup>1,6,20–23,35,39</sup> Therefore, our findings based on experimental results provide two important insights into the toughness of DN gels. First, the dissipation in the pre-yielding zone, as well as in the yielding zone, makes a large contribution to  $\Gamma_{\text{diss}}$ . Previously, most studies on DN gels focused on energy dissipation only in the yielding zone because the energy dissipation density ( $\text{J m}^{-3}$ ) in the pre-yielding zone is relatively small; thus, it was considered negligible. However, our results indicate that  $\Gamma_{\text{diss}}$  in the pre-yielding zone is comparable to or even larger than that in the yielding zone. This is because the dissipation volume ( $\text{m}^3$ ) in the pre-yielding zone is significantly larger than that in the yielding zone. Specifically, for the DN gel used in this work, the dissipative volume ( $\text{m}^3$ ) and the average dissipated energy density ( $\text{J m}^{-3}$ ) in the pre-yielding region are  $\sim 10$  times larger and  $\sim 10$  times smaller than those in the yield region, respectively; thus, the two regions make similar contribution to  $\Gamma_{\text{diss}}$ .

Second, we experimentally found that the intrinsic fracture energy  $\Gamma_0$  is not as small as  $\sim 10^1 \text{ J m}^{-2}$ , which has been assumed in previous reports,<sup>20,21</sup> but rather is in the order of  $\sim 10^2 \text{ J m}^{-2}$  or larger. Our results further imply that the intrinsic fracture energy  $\Gamma_0$  is higher than that of the second network,  $\Gamma_{2\text{nd}}$ . This is reasonable because not all strands of the first network are broken, even if a DN gel is largely deformed until rupture. If all first-network strands could be broken, some mechanical properties, such as stress at rupture in tensile test would be the same as those for the second network. In fact, it is known that the stress at the breaking point of a DN gel is much higher than that of the second-network single-network gel.<sup>22,27,37,56</sup> Nakajima et al. suggested that only  $\sim 10\%$  of the first-network strands are broken at the rupture point of a DN gel under uniaxial tension from mechanical hysteresis characterization.<sup>36</sup> Matsuda et al. detected the

chain scission in a yielded DN gel being in the order of  $10^{-2} \text{ mol m}^{-3}$  by mechanochemical ferrous oxidation technique.<sup>37</sup> Considering that the number density of the first network strands is  $\nu_{1st} \approx 0.16 \text{ mol m}^{-3}$ , the fraction of the broken first-network strands is estimated to be in the order of  $\sim 10\%$ . (Note that  $\nu_{1st}$  was estimated from  $\nu_{1st} = E_0/3k_B T N_A Q$  under the assumption of affine network theory, where  $E_0 = 26 \text{ kPa}$  is the tensile elastic modulus of the first-network gel at the preparation state,  $k_B$  is the Boltzmann constant,  $T = 298 \text{ K}$  is the absolute temperature,  $N_A$  is the Avogadro constant, and  $Q = 22$  is the volumetric swelling ratio of the first network from the preparation state to the state in the DN gel used in the literature.<sup>37</sup>) These two individual results<sup>36,37</sup> suggest that most (probably  $\sim 90\%$ ) of the first network strands are not broken even under large deformation above yielding. Also, another recent paper by Chen et al. shows that the first network strands in a quadruplet-network elastomer are still considerably loaded in the necked part after yielding, revealed using spiropyran mechanophore incorporated as the first network crosslinker.<sup>57</sup> Therefore, it is plausible that the surviving first-network strands (supposedly disconnected clusters of the broken first network<sup>22,36,50,58</sup>) play a role in strengthening and toughening damaged DN gels that have already experienced significant internal fracturing. The role of the surviving first network should be revealed in the future. In our opinion, the possible physical picture is either or combination of the following mechanisms. (1) The broken first network clusters could act as fillers that restrict or divert the crack growth, similar to some composite or micro-structured materials.<sup>59–63</sup> (2) Upon the crack growth, some of the surviving first network strands can be ruptured very near the crack tip (e.g.  $10^2$ – $10^4 \text{ nm}$  region from the tip) inside of the gel and/or at the surface of the crack, which dissipates further energy. This mechanism could be interpreted as the further internal fracturing; however, it should be a crack-tip-specific phenomenon since most (probably  $\sim 90\%$ ) of the first-network

strands cannot be ruptured upon the homogeneous deformation. (3) Internal fracturing of *the second network* would be also induced under large stress with the presence of the surviving first network. (4) The second network might exhibit strain-induced intermolecular interaction that enhances the crack-tip toughness, similar to the strain-induced crystallization of slide-ring PEG gels and tri-branched PEG gels at relatively high polymer concentration.<sup>15,64</sup> Since PAAm has hydrogen bonding donor and acceptor capabilities, the aligned PAAm strands would possibly interact with each other to form amorphous bundles or crystals. The second network alignment could be enhanced by the first network clusters that may act as giant sliding crosslinkers.<sup>22</sup>

The effect of the broken first network on the crack-tip toughness  $\Gamma_0$  is an important aspect when studying the fracture mechanics of DN gels because  $\Gamma_0$  contributes not only to restricting an initiation of the crack propagation at the crack tip but also to enhancing  $\Gamma_{\text{diss}}$  by increasing the damage zone size upon deformation.<sup>20,21,54</sup>

The finding of  $\Gamma_0 > \Gamma_{2\text{nd}}$  might be valid for other interpenetrated network materials. For example, Zhang et al. reported that the intrinsic fracture energy of an alginate/PAAm DN gel (fracture energy  $\Gamma = 1063 \text{ J m}^{-2}$ ) is  $\Gamma_0 \approx 400 \text{ J m}^{-2}$ , which is characteristic of pre-stretched samples.<sup>54</sup> Although they did not compare the  $\Gamma_0$  with the fracture energy of the second network  $\Gamma_{2\text{nd}}$ , we expect that  $\Gamma_{2\text{nd}}$  for the PAAm network in their work (PAAm  $\sim 10 \text{ wt.}\%$  and MBAA crosslinker  $\sim 0.08 \text{ mol}\%$  with respect to the AAm monomer unit)<sup>54</sup> is  $100 \text{ J m}^{-2}$  or lower. This estimation is based on the fact that the fracture energy of a PAAm gel with a higher polymer content and a lower crosslinker density (PAAm  $\sim 14 \text{ wt.}\%$  and MBAA crosslinker  $\sim 0.05 \text{ mol}\%$  with respect to the AAm monomer unit) synthesized via a similar polymerization procedure in their work (1-



hour UV irradiation in the presence of ammonium persulphate and *N,N,N',N'*-tetramethylethylenediamine) showed a fracture energy of  $100 \text{ J m}^{-2}$ .<sup>10</sup>

We have concluded that the fracture energy of the DN gel used in this work ( $\Gamma \approx 900 \text{ J m}^{-2}$ ) consists of contributions of  $\Gamma_{\text{diss}}$  in the yielding zone of  $50\text{--}300 \text{ J m}^{-2}$ ,  $\Gamma_{\text{diss}}$  in the pre-yielding zone of  $200\text{--}400 \text{ J m}^{-2}$ , and an intrinsic fracture energy  $\Gamma_0$  of  $150\text{--}700 \text{ J m}^{-2}$ . It should be mentioned that the fracture energy of the DN gel ( $\sim 900 \text{ J m}^{-2}$ ) is a moderate value of the fracture energies of common DN gels synthesized in various compositions (typically  $300\text{--}5000 \text{ J m}^{-2}$ ).<sup>30,31</sup> The ratio of the three contributions should vary according to the composition of the DN gel, which needs to be investigated further.

## CONCLUSION

Energy dissipation in the damage zone around the crack tip of the DN gel characterized by mechanochemical technique was quantitatively compared with the fracture energy. The results show that energy dissipation by internal fracturing in the damage zone,  $\Gamma_{\text{diss}}$  ( $\sim 400 \text{ J m}^{-2}$ ), is considerably smaller than the fracture energy  $\Gamma$  as characterized by the tearing test ( $\sim 900 \text{ J m}^{-2}$ ), suggesting that the intrinsic fracture energy  $\Gamma_0$  is not negligibly small. This prediction was further confirmed by characterizing the fracture energies of the PAAm single-network gel ( $\sim 200 \text{ J m}^{-2}$ ) and a largely pre-stretched DN gel ( $\sim 700 \text{ J m}^{-2}$ ). These results also suggest that  $\Gamma_0$  is larger than the fracture energy of the second network. We also clarified that the energy dissipation around the crack tip of the DN gel in the pre-yielding zone is comparable to or larger than that in the yielding zone, although dissipation density per unit volume is relatively small, because the dissipative volume in the pre-yielding zone is much larger. These results suggest for the first time that the contributions to the energy dissipation cannot only be found in the yielding zone but also in the pre-yielding zone and that the intrinsic fracture energy contributes considerably to the large fracture energy of DN gels.

The non-negligible contributions of the dissipation in the pre-yielding zone and/or intrinsic fracture energy being higher than the stretchable-network fracture energy would explain the toughening effect of some double- and triple-network gels and elastomers that do not show explicit yielding and large extensibility.<sup>12,27,30,31</sup> Each contribution to the fracture energy is important not only to understand the toughening mechanisms of multiple-network materials but also to optimize their mechanical properties for targeted applications. Furthermore, the large intrinsic fracture energy  $\Gamma_0$  after elimination of the damage-zone dissipation capacity is also

suggestive in practice since it had been often viewed that DN gels with the irreversible sacrificial bond mechanism were no longer ‘tough’ after the first deformation.<sup>10,11,15</sup> Our results as well as some reported results<sup>54,65</sup> indicate that the multiple-network soft materials are intrinsically tough even after the bulk dissipation, presumably because of the surviving first-network strands.

## ASSOCIATED CONTENT

### Supporting Information

The Supporting Information is available.

Experimental setup of the trouser-fracture test (Figure S1); single-edge notch tests of the virgin DN gel, pre-stretched DN gel and PAAm gels (Supporting Note I and Figures S2–S4); trouser-tearing tests of the PAAm gels (Supporting Note I and Figure S5); potential errors in the fluorescence method using mechanoradical polymerization (Supporting Note II) (PDF)

## AUTHOR INFORMATION

### Corresponding Authors

\*E-mail: [tkhr.matsuda@gmail.com](mailto:tkhr.matsuda@gmail.com) (T.M.); [gong@sci.hokudai.ac.jp](mailto:gong@sci.hokudai.ac.jp) (J.P.G.).

### ORCID

Takahiro Matsuda: [orcid.org/0000-0001-9681-8007](https://orcid.org/0000-0001-9681-8007)

Runa Kawakami: Not available

Tasuku Nakajima: [orcid.org/0000-0002-2235-3478](https://orcid.org/0000-0002-2235-3478)

Yukiko Hane: Not available

JianPing Gong: [orcid.org/0000-0003-2228-2750](https://orcid.org/0000-0003-2228-2750)

## **Note**

The authors declare no competing financial interests.

## **ACKNOWLEDGMENT**

This research was partially funded by a Grant-in-Aid for JSPS Research Fellows (No. 17J09290) and for Scientific Research (S) (No. 17H06144) from the Japan Society for the Promotion of Science, and by the ImPACT Program of the Council for Science, Technology and Innovation (Cabinet Office, Government of Japan). The authors thank Toagosei Co., Ltd. for providing NaAMPS. R.K. and T.M. thank the Nikon Imaging Center at Hokkaido University and Kentaro Kobayashi for their assistance with laser-scanning confocal microscopy.

## REFERENCES

- (1) Long, R.; Hui, C.-Y.; Gong, J. P.; Bouchbinder, E. The fracture of highly deformable soft materials: A tale of two length scales. *Annu. Rev. Condens. Matter Phys.* **2021**, *12*, 71–94. DOI: 10.1146/annurev-conmatphys-042020-023937
- (2) Zhao, X.; Chen, X.; Yuk, H.; Lin, S.; Liu, X.; Parada, G. Soft materials by design: Unconventional polymer networks give extreme properties. *Chem. Rev.* **2021**, *121*, 4309–4372. DOI: 10.1021/acs.chemrev.0c01088
- (3) Bai, R.; Yang, J.; Suo, Z. Fatigue of hydrogels. *Eur. J. Mech. A Solids* **2019**, *74*, 337–370. DOI: 10.1016/j.euromechsol.2018.12.001
- (4) Creton, C. 50th anniversary perspective: Networks and gels: Soft but dynamic and tough. *Macromolecules* **2017**, *50*, 8297–8316. DOI: 10.1021/acs.macromol.7b01698
- (5) Creton, C.; Ciccotti, M. Fracture and adhesion of soft materials: A review. *Rep. Prog. Phys.* **2016**, *79*, 046601. DOI: 10.1088/0034-4885/79/4/046601
- (6) Long, R.; Hui, C. Y. Fracture toughness of hydrogels: Measurement and interpretation. *Soft Matter* **2016**, *12*, 8069–8086. DOI: 10.1039/C6SM01694D
- (7) Zhao, X. Multi-scale multi-mechanism design of tough hydrogels: Building dissipation into stretchy networks. *Soft Matter* **2014**, *10*, 672–687. DOI: 10.1039/C3SM52272E
- (8) Haraguchi, K.; Takehisa, T. Nanocomposite hydrogels: A unique organic-inorganic network structure with extraordinary mechanical, optical, and swelling/de-swelling properties. *Adv. Mater.* **2002**, *14*, 1120–1124. DOI: 10.1002/1521-4095(20020816)14:16<1120::AID-ADMA1120>3.0.CO;2-9
- (9) Gong, J. P.; Katsuyama, Y.; Kurokawa, T.; Osada, Y. Double-network hydrogels with extremely high mechanical strength. *Adv. Mater.* **2003**, *15*, 1155–1158. DOI: 10.1002/adma.200304907

- (10) Sun, J. Y.; Zhao, X.; Illeperuma, W. R. K.; Chaudhuri, O.; Oh, K. H.; Mooney, D. J.; Vlassak, J. J.; Suo, Z. Highly stretchable and tough hydrogels. *Nature* **2012**, *489*, 133–136. DOI: 10.1038/nature11409
- (11) Sun, T. L.; Kurokawa, T.; Kuroda, S.; Ihsan, A. B.; Akasaki, T.; Sato, K.; Haque, M. A.; Nakajima, T.; Gong, J. P. Physical hydrogels composed of polyampholytes demonstrate high toughness and viscoelasticity. *Nat. Mater.* **2013**, *12*, 932–937. DOI: 10.1038/nmat3713
- (12) Ducrot, E.; Chen, Y.; Bulters, M.; Sijbesma, R. P.; Creton, C. Toughening elastomers with sacrificial bonds and watching them break. *Science* **2014**, *344*, 186–189. DOI: 10.1126/science.1248494
- (13) Lin, S.; Liu, X.; Liu, J.; Yuk, H.; Loh, H. C.; Parada, G. A.; Settens, C.; Song, J.; Masic, A.; McKinley, G. H.; Zhao, X. Anti-fatigue-fracture hydrogels. *Sci. Adv.* **2019**, *5*, eaau8528. DOI: 10.1126/sciadv.aau8528
- (14) Hua, M.; Wu, S.; Ma, Y.; Zhao, Y.; Chen, Z.; Frenkel, I.; Strzalka, J.; Zhou, H.; Zhu, X.; He, X. Strong tough hydrogels via the synergy of freeze-casting and salting out. *Nature* **2021**, *590*, 594–599. DOI: 10.1038/s41586-021-03212-z
- (15) Liu, C.; Morimoto, N.; Jiang, L.; Kawahara, S.; Noritomi, T.; Yokoyama, H.; Mayumi, K.; Ito, K. Tough hydrogels with rapid self-reinforcement. *Science* **2021**, *372*, 1078–1081. DOI: 10.1126/science.aaz6694
- (16) Rogers, J. A.; Someya, T.; Huang, Y. Materials and mechanics for stretchable electronics. *Science* **2010**, *327*, 1603–1607. DOI: 10.1126/science.1182383
- (17) Lim, H.-R.; Kim, H. S.; Qazi, R.; Kwon, Y. T.; Jeong, J.-W.; Yeo, W.-H. Advanced soft materials, sensor integrations, and applications of wearable flexible hybrid electronics in healthcare, energy, and environment. *Adv. Mater.* **2020**, *32*, 1901924. DOI: 10.1002/adma.201901924
- (18) Fuchs, S.; Shariati, K.; Ma, M. Specialty tough hydrogels and their biomedical applications. *Adv. Healthc. Mater.* **2020**, *9*, 1901396. DOI: 10.1002/adhm.201901396

- (19) Annabi, N.; Tamayol, A.; Uquillas, J. A.; Akbari, M.; Bertassoni, L. E.; Cha, C.; Camci-Unal, G.; Dokmeci, M. R.; Peppas, N. A.; Khademhosseini, A. 25th anniversary article: Rational design and applications of hydrogels in regenerative medicine. *Adv. Mater.* **2014**, *26*, 85–123. DOI: 10.1002/adma.201303233
- (20) Tanaka, Y. A local damage model for anomalous high toughness of double-network gels. *Europhys. Lett.* **2007**, *78*, 56005. DOI: 10.1209/0295-5075/78/56005
- (21) Brown, H. R. A model of the fracture of double network gels. *Macromolecules* **2007**, *40*, 3815–3818. DOI: 10.1021/ma062642y
- (22) Gong, J. P. Why are double network hydrogels so tough? *Soft Matter* **2010**, *6*, 2583–2590. DOI: 10.1039/B924290B
- (23) Nakajima, T. Generalization of the sacrificial bond principle for gel and elastomer toughening. *Polym. J.* **2017**, *49*, 477–485. DOI: 10.1038/pj.2017.12
- (24) Chen, Q.; Chen, H.; Zhu, L.; Zheng, J. Fundamentals of double network hydrogels. *J. Mater. Chem. B* **2015**, *3*, 3654–3676. DOI: 10.1039/C5TB00123D
- (25) Nakajima, T.; Sato, H.; Zhao, Y.; Kawahara, S.; Kurokawa, T.; Sugahara, K.; Gong, J. P. A universal molecular stent method to toughen any hydrogels based on double network concept. *Adv. Funct. Mater.* **2012**, *22*, 4426–4432. DOI: 10.1002/adfm.201200809
- (26) Murai, J.; Nakajima, T.; Matsuda, T.; Tsunoda, K.; Nonoyama, T.; Kurokawa, T.; Gong, J. P. Tough double network elastomers reinforced by the amorphous cellulose network. *Polymer* **2019**, *178*, 121686. DOI: 10.1016/j.polymer.2019.121686
- (27) Matsuda, T.; Nakajima, T.; Gong, J. P. Fabrication of tough and stretchable hybrid double-network elastomers using ionic dissociation of polyelectrolyte in nonaqueous media. *Chem. Mater.* **2019**, *31*, 3766–3776. DOI: 10.1021/acs.chemmater.9b00871
- (28) Nakajima, T.; Ozaki, Y.; Namba, R.; Ota, K.; Maida, Y.; Matsuda, T.; Kurokawa, T.; Gong, J. P. Tough double-network gels and elastomers from the nonprestretched first network. *ACS Macro Lett.* **2019**, *8*, 1407–1412. DOI: 10.1021/acsmacrolett.9b00679

- (29) Tanaka, Y.; Kuwabara, R.; Na, Y. H.; Kurokawa, T.; Gong, J. P.; Osada, Y. Determination of fracture energy of high strength double network hydrogels. *J. Phys. Chem. B* **2005**, *109*, 11559–11562. DOI: 10.1021/jp0500790
- (30) Ahmed, S.; Nakajima, T.; Kurokawa, T.; Anamul Haque, M.; Gong, J. P. Brittle–ductile transition of double network hydrogels: Mechanical balance of two networks as the key factor. *Polymer* **2014**, *55*, 914–923. DOI: 10.1016/j.polymer.2013.12.066
- (31) Nakajima, T.; Kurokawa, T.; Furukawa, H.; Gong, J. P. Effect of the constituent networks of double-network gels on their mechanical properties and energy dissipation process. *Soft Matter* **2020**, *16*, 8618–8627. DOI: 10.1039/D0SM01057J
- (32) Na, Y.-H.; Tanaka, Y.; Kawauchi, Y.; Furukawa, H.; Sumiyoshi, T.; Gong, J. P.; Osada, Y. Necking phenomenon of double-network gels. *Macromolecules* **2006**, *39*, 4641–4645. DOI: 10.1021/ma060568d
- (33) Matsuda, T.; Nakajima, T.; Fukuda, Y.; Hong, W.; Sakai, T.; Kurokawa, T.; Chung, U.-I.; Gong, J. P. Yielding criteria of double network hydrogels. *Macromolecules* **2016**, *49*, 1865–1872. DOI: 10.1021/acs.macromol.5b02592
- (34) Webber, R. E.; Creton, C.; Brown, H. R.; Gong, J. P. Large strain hysteresis and Mullins effect of tough double-network hydrogels. *Macromolecules* **2007**, *40*, 2919–2927. DOI: 10.1021/ma062924y
- (35) Yu, Q. M.; Tanaka, Y.; Furukawa, H.; Kurokawa, T.; Gong, J. P. Direct observation of damage zone around crack tips in double-network gels. *Macromolecules* **2009**, *42*, 3852–3855. DOI: 10.1021/ma900622s
- (36) Nakajima, T.; Kurokawa, T.; Ahmed, S.; Wu, W.-L.; Gong, J. P. Characterization of internal fracture process of double network hydrogels under uniaxial elongation. *Soft Matter* **2013**, *9*, 1955–1966. DOI: 10.1039/C2SM27232F
- (37) Matsuda, T.; Kawakami, R.; Namba, R.; Nakajima, T.; Gong, J. P. Mechanoresponsive self-growing hydrogels inspired by muscle training. *Science* **2019**, *363*, 504–508. DOI: 10.1126/science.aau9533



- (38) Tanaka, Y.; Kawauchi, Y.; Kurokawa, T.; Furukawa, H.; Okajima, T.; Gong, J. P. Localized yielding around crack tips of double-network gels. *Macromol. Rapid Commun.* **2008**, *29*, 1514–1520. DOI: 10.1002/marc.200800227
- (39) Liang, S.; Wu, Z. L.; Hu, J.; Kurokawa, T.; Yu, Q. M.; Gong, J. P. Direct observation on the surface fracture of ultrathin film double-network hydrogels. *Macromolecules* **2011**, *44*, 3016–3020. DOI: 10.1021/ma2000527
- (40) Matsuda, T.; Kawakami, R.; Nakajima, T.; Gong, J. P. Crack tip field of a double-network gel: Visualization of covalent bond scission through mechanoradical polymerization. *Macromolecules* **2020**, *53*, 8787–8795. DOI: 10.1021/acs.macromol.0c01485
- (41) Sloopman, J.; Waltz, V.; Yeh, C. J.; Baumann, C.; Göstl, R.; Comtet, J.; Creton, C. Quantifying rate- and temperature-dependent molecular damage in elastomer fracture. *Phys. Rev. X* **2020**, *10*, 041045. DOI: 10.1103/PhysRevX.10.041045
- (42) Chen, Y.; Yeh, C. J.; Qi, Y.; Long, R.; Creton, C. From force-responsive molecules to quantifying and mapping stresses in soft materials. *Sci. Adv.* **2020**, *6*, eaaz5093. DOI: 10.1126/sciadv.aaz5093
- (43) Nakajima, T.; Furukawa, H.; Tanaka, Y.; Kurokawa, T.; Osada, Y.; Gong, J. P. True chemical structure of double network hydrogels. *Macromolecules* **2009**, *42*, 2184–2189. DOI: 10.1021/ma802148p
- (44) Rivlin, R. S.; Thomas, A. G. Rupture of rubber. I. Characteristic energy for tearing. *J. Polym. Sci.* **1953**, *10*, 291–318. DOI: 10.1002/pol.1953.120100303
- (45) Greensmith, H. W.; Thomas, A. G. Rupture of rubber. III. Determination of tear properties. *J. Polym. Sci.* **1955**, *18*, 189–200. DOI: 10.1002/pol.1955.120188803
- (46) Greensmith, H. W. Rupture of rubber. X. The change in stored energy on making a small cut in a test piece held in simple extension. *J. Appl. Polym. Sci.* **1963**, *7*, 993–1002. DOI: 10.1002/app.1963.070070316

- (47) Lindley, P. B. Energy for crack growth in model rubber components. *J. Strain Anal.* **1972**, *7*, 132–140. DOI: 10.1243/03093247V072132
- (48) Millereau, P.; Ducrot, E.; Clough, J. M.; Wiseman, M. E.; Brown, H. R.; Sijbesma, R. P.; Creton, C. Mechanics of elastomeric molecular composites. *Proc. Natl. Acad. Sci. U.S.A.* **2018**, *115*, 9110–9115. DOI: 10.1073/pnas.1807750115
- (49) Fukao, K.; Nakajima, T.; Nonoyama, T.; Kurokawa, T.; Kawai, T.; Gong, J. P. Effect of relative strength of two networks on the internal fracture process of double network hydrogels as revealed by *in situ* small-angle X-ray scattering. *Macromolecules* **2020**, *53*, 1154–1163. DOI: 10.1021/acs.macromol.9b02562
- (50) Guo, H.; Hong, W.; Kurokawa, T.; Matsuda, T.; Wu, Z. L.; Nakajima, T.; Takahata, M.; Sun, T.; Rao, P.; Gong, J. P. Internal damage evolution in double-network hydrogels studied by microelectrode technique. *Macromolecules* **2019**, *52*, 7114–7122. DOI: 10.1021/acs.macromol.9b01308
- (51) Tanaka, Y.; Fukao, K.; Miyamoto, Y. Fracture energy of gels. *Eur. Phys. J. E* **2000**, *3*, 395–401. DOI: 10.1007/s101890070010
- (52) Zhang, E.; Bai, R.; Morelle, X. P.; Suo, Z. Fatigue fracture of nearly elastic hydrogels. *Soft Matter* **2018**, *14*, 3563–3571. DOI: 10.1039/C8SM00460A
- (53) Yang, C.; Yin, T.; Suo, Z. Polyacrylamide hydrogels. I. Network imperfection. *J. Mech. Phys. Solids* **2019**, *131*, 43–55. DOI: 10.1016/j.jmps.2019.06.018
- (54) Zhang, T.; Lin, S.; Yuk, H.; Zhao, X. Predicting fracture energies and crack-tip fields of soft tough materials. *Extreme Mech. Lett.* **2015**, *4*, 1–8. DOI: 10.1016/j.eml.2015.07.007
- (55) Mai, T. -T.; Matsuda, T.; Nakajima, T.; Gong, J. P.; Urayama, K. Damage cross-effect and anisotropy in tough double network hydrogels revealed by biaxial stretching. *Soft Matter*, **2019**, *15*, 3719–3732. DOI: 10.1039/c9sm00409b

- (56) Itagaki, H.; Kurokawa, T.; Furukawa, H.; Nakajima, T.; Katsumoto, Y.; Gong, J. P. Water-induced brittle-ductile transition of double network hydrogels. *Macromolecules* **2010**, *43*, 9495–9500. DOI: 10.1021/ma101413j
- (57) Chen, Y.; Sanoja, G.; Creton, C. Mechanochemistry unveils stress transfer during sacrificial bond fracture of tough multiple network elastomers. *Chem. Sci.* **2021**, *12*, 11098–11108. DOI: 10.1039/D1SC03352B
- (58) Morovati, V.; Saadat, M. A.; Dargazany, R. Necking of double-network gels: Constitutive modeling with microstructural insight. *Phys. Rev. E* **2020**, *102*, 062501. DOI: 10.1103/PhysRevE.102.062501
- (59) Mirkhalaf, M.; Dastjerdi, A.; Barthelat, F. Overcoming the brittleness of glass through bio-inspiration and micro-architecture. *Nat Commun* **2014**, *5*, 3166. DOI: 10.1038/ncomms4166
- (60) Magrini, T.; Moser, S.; Fellner, M.; Lauria, A.; Bouville, F.; Studart, A. R. Transparent nacre-like composites toughened through mineral bridges. *Adv. Funct. Mater.* **2020**, *30*, 2002149. DOI: 10.1002/adfm.202002149
- (61) Mesgarnejad, A.; Pan, C.; Erb, R. M.; Shefelbine, S. J.; Karma, A. Crack path selection in orientationally ordered composites. *Phys. Rev. E.* **2020**, *102*, 013004. DOI: 10.1103/PhysRevE.102.013004
- (62) Lin, S.; Liu, J.; Liu, X.; Zhao, X. Muscle-like fatigue-resistant hydrogels by mechanical training. *Proc. Natl. Acad. Sci. U.S.A.* **2019**, *116*, 10244–10249. DOI: 10.1073/pnas.1903019116
- (63) Zheng, Y.; Kiyama, R.; Matsuda, T.; Cui, K.; Li, X.; Cui, W.; Guo, Y.; Nakajima, T.; Kurokawa, T.; Gong, J. P. Nanophase separation in immiscible double network elastomers induces synergetic strengthening, toughening, and fatigue resistance. *Chem. Mater.* **2021**, *33*, 3321–3334. DOI: 10.1021/acs.chemmater.1c00512
- (64) Fujiyabu, T.; Sakumichi, N.; Katashima, T.; Liu, C.; Mayumi, K.; Chung, U.; Sakai, T. Tri-branched gels: Low branching factors make rubbery materials ultra-elastic. **2021**,

arXiv:2106.13424. arXiv.org e-Print archive. <https://arxiv.org/abs/2106.13424> (accessed Aug 28, 2021).

(65) Lin, S.; Zhou, Y.; Zhao, X. Designing extremely resilient and tough hydrogels via delayed dissipation. *Extreme Mech. Lett.* 2014, *1*, 70–75. DOI: 10.1016/j.eml.2014.11.002